Electronic Supplementary Material (ESI) for RSC Advances.
This journal is © The Royal Society of Chemistry 2024

Supplementary Information

Influence of Halogen-Halogen Interactions in the Self-Assembly of Pillar[5]arene-Based Supramolecular Polymers

Mickey Vinodh, Anwar A. Alshammari and Talal F. Al-Azemi*
Chemistry Department, Kuwait University, P.O. Box 5969, Safat 13060, Kuwait

Table of contents

* Corresponding author.
E-mail address: t.alazemi@ku.edu.kw.

Single crystal X-ray diffraction analysis:

Table S1. Crystal data and experimental parameters of the structural analysis of [**DMP5 ⊃ DFB**]and [**DMP5 ⊃ DCB**].

Crystal sample	**[DMP5 ⊃ DFB]**	**[DMP5 ⊃ DCB]**
Chemical formula	$C_{49}H_{58}F_2O_{10}$	$C_{53}H_{66}Cl_4O_{10}$
M_r	844.95	1004.85
Crystal system, space group	Tetragonal, $I4_1/a$	Triclinic, P-1
Temperature (K)	150	296
a, b, c (Å)	15.0762 (13), 15.0762 (13), 39.5384 (15)	10.2873 (3), 12.1713 (4), 22.7710 (8)
α, β, γ (°)	90, 90, 90	90.681 (2), 98.012 (2), 109.405 (2)
V (Å^3)	8986.7 (16)	2657.76 (15)
Z	8	2
Radiation type	Mo $K\alpha$	Cu $K\alpha$
μ (mm^{-1})	0.09	2.47
Crystal size (mm)	0.20 × 0.18 × 0.17	0.25 × 0.21 × 0.15
Diffractometer	Rigaku R-AXIS RAPID	Bruker *APEX*-II CCD
Absorption correction	Multi-scan *ABSCOR* (Rigaku, 1995)	Multi-scan *SADABS2016*/2 - Bruker AXS area detector scaling and absorption correction
T_{min}, T_{max}	0.665, 0.985	0.57, 0.71
No. of measured, independent & observed [$I > 2\sigma(I)$] reflections	36777, 3949, 2547	24970, 9182, 6770
R_{int}	0.056	0.036
$(\sin\theta/\lambda)_{max}$ (Å^{-1})	0.595	0.595
$R[F^2 > 2\sigma(F^2)]$, $wR(F^2)$, S	0.070, 0.226, 1.04	0.072, 0.224, 1.02
No. of reflections	3949	9182
No. of parameters	281	642
No. of restraints	20	70
H-atom treatment	Constrained	Constrained

$\Delta\rho_{max}$, $\Delta\rho_{min}$ (e Å^{-3})	0.50, −0.29	0.53, −0.46

Table S1. Crystal data and experimental parameters of the structural analysis of [**DMP5 ⊃ DBB**]and [**DMP5 ⊃ DIB**].

Crystal sample	**[DMP5 ⊃ DBB]**	**[DMP5 ⊃ DIB]**
Chemical formula	$C_{53}H_{66}Br_4O_{10}$	$C_{104}H_{128}I_7O_{20}$
M_r	1182.69	2586.36
Crystal system, space group	Triclinic, *P*-1	Triclinic, *P*-1
Temperature (K)	150	150
a, *b*, *c* (Å)	10.3567 (8), 12.1184 (9), 22.4299 (15)	10.6280 (9), 12.2335 (12), 23.534 (2)
α, β, γ (°)	91.283 (6), 95.977 (7), 110.754 (8)	88.021 (6), 77.859 (6), 71.497 (5)
V (Å^3)	2612.8 (3)	2835.1 (5)
Z	2	1
Radiation type	Mo *K*α	Mo *K*α
μ (mm^{-1})	3.14	1.98
Crystal size (mm)	0.25 × 0.05 × 0.04	0.16 × 0.11 × 0.06
Diffractometer	Rigaku R-AXIS RAPID	Rigaku R-AXIS RAPID
Absorption correction	Multi-scan *ABSCOR* (Rigaku, 1995)	Multi-scan *ABSCOR* (Rigaku, 1995)
T_{min}, T_{max}	0.388, 0.882	0.542, 0.873
No. of measured, independent & observed [$I > 2\sigma(I)$] reflections	18256, 9072, 4246	34070, 9826, 4559
R_{int}	0.087	0.067
$(\sin\theta/\lambda)_{max}$ (Å^{-1})	0.595	0.595
$R[F^2 > 2\sigma(F^2)]$, $wR(F^2)$, S	0.065, 0.179, 0.91	0.120, 0.399, 1.23
No. of reflections	9072	9826
No. of parameters	614	651
No. of restraints	577	151
H-atom treatment	Constrained	Constrained
$\Delta\rho_{max}$, $\Delta\rho_{min}$ (e Å^{-3})	1.16, −1.10	1.66, −1.12

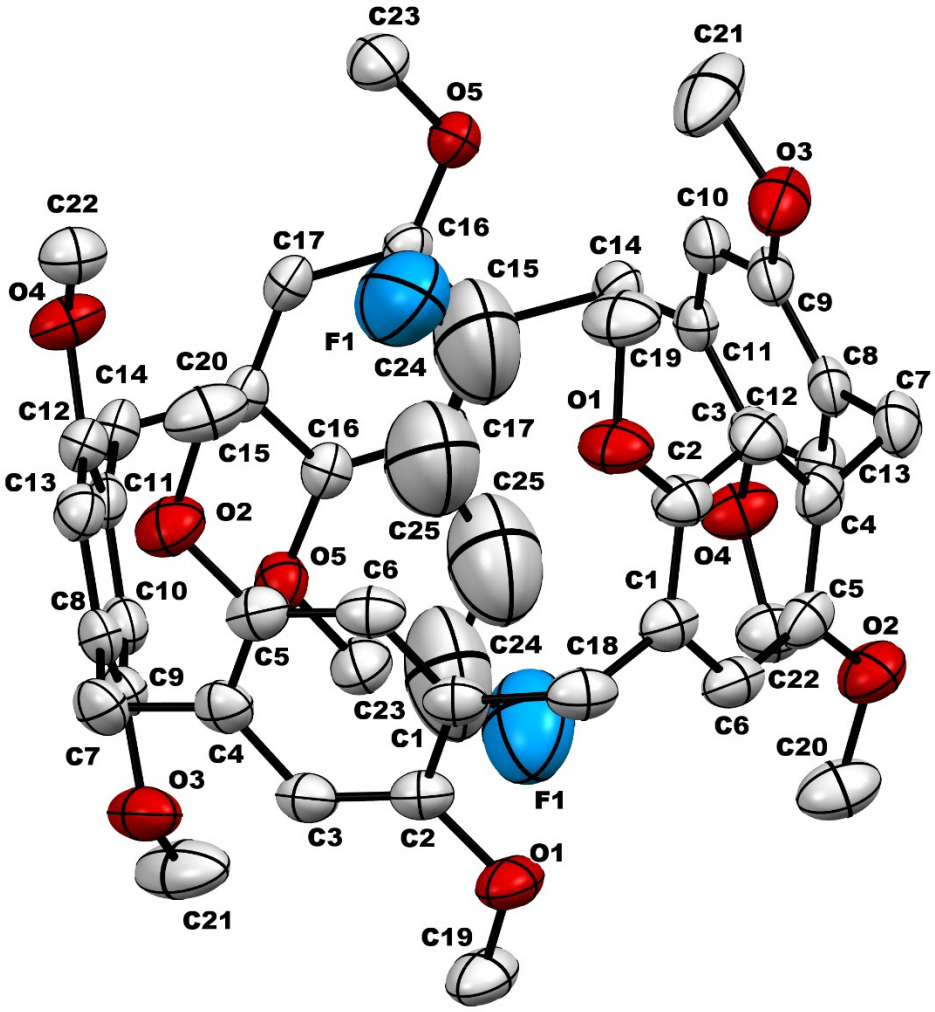

Figure S1. Thermal ellipsoid representation (30% probability) **of** DPM5⊃BuF2 crystal (Hydrogen atoms are hided for clarity)

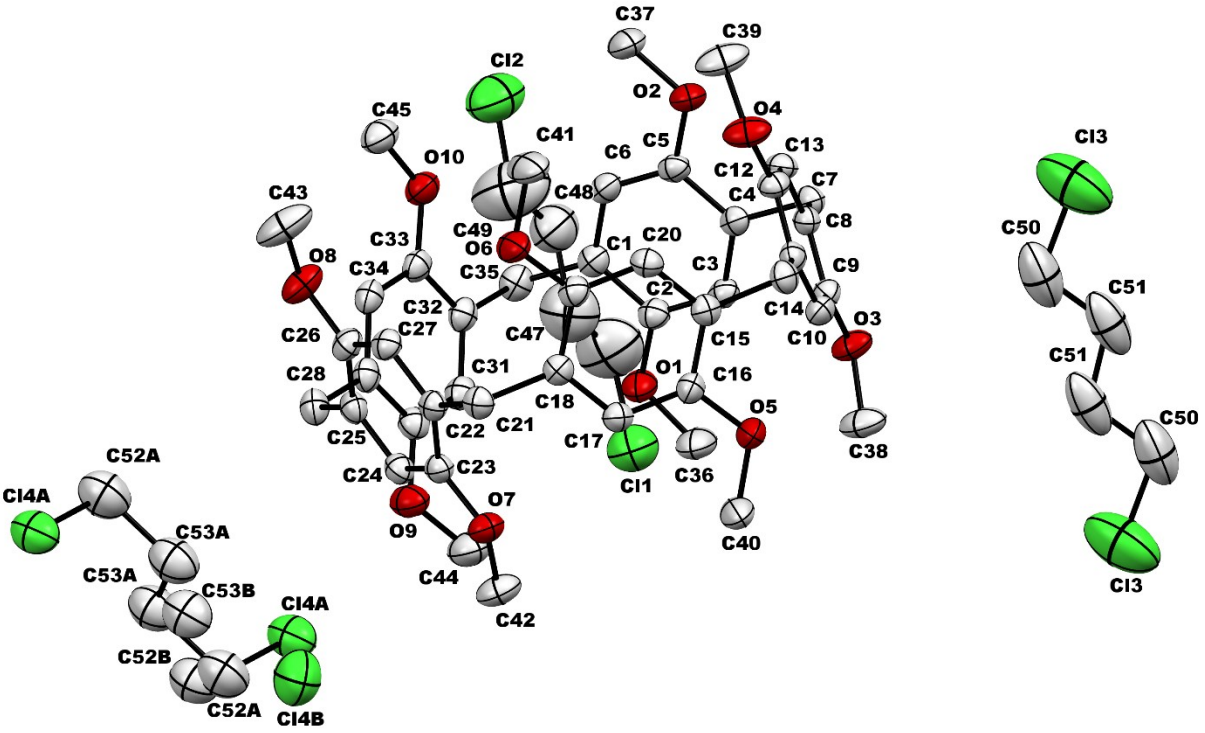

Figure S2. Thermal ellipsoid representation (30% probability) **of** DPM5⊃BuCl2 crystal (Hydrogen atoms are hided for clarity)

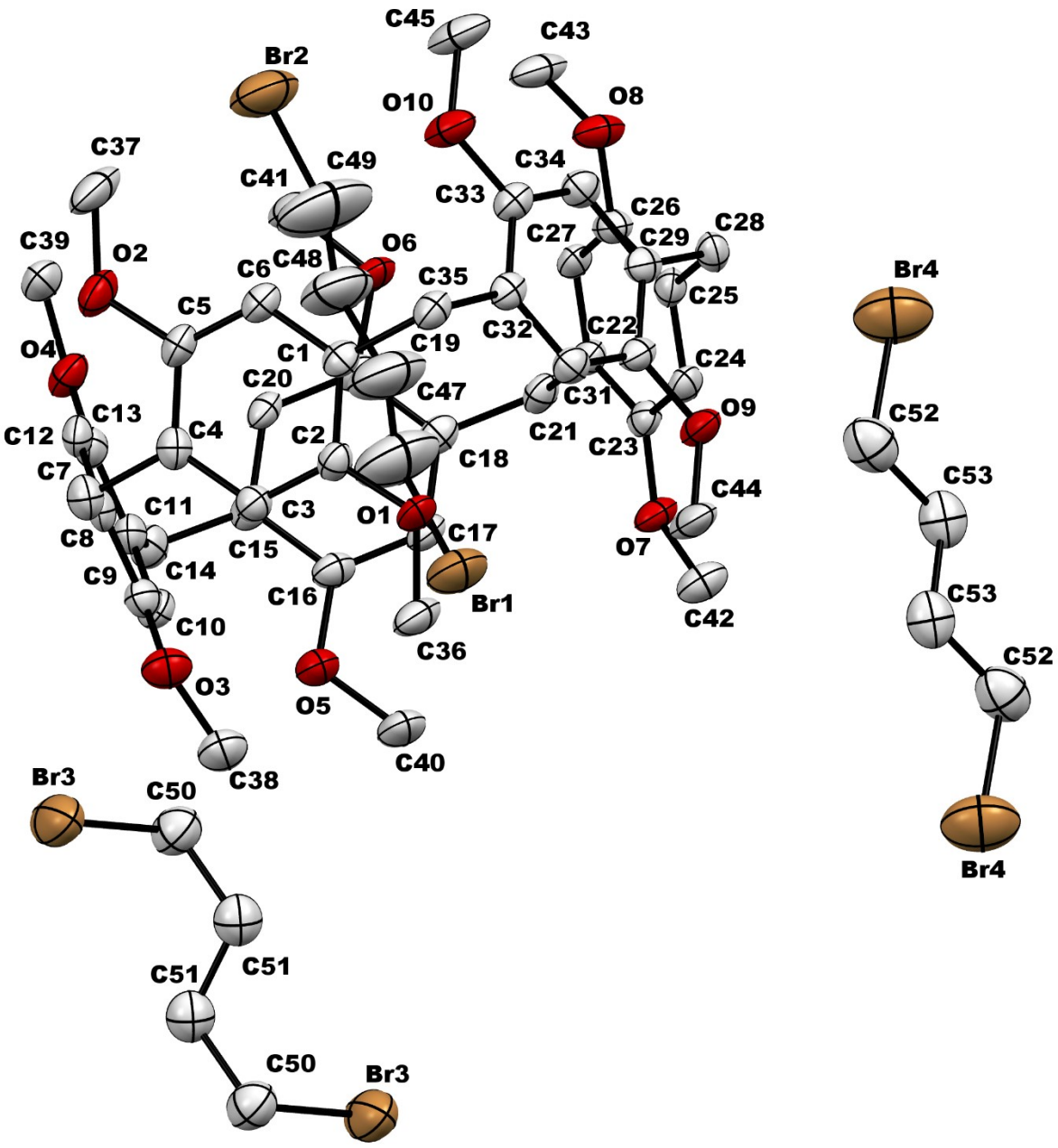

Figure S3. Thermal ellipsoid representation (50% probability) **of** DPM5⊃BuBr2 crystal (Hydrogen atoms are hided for clarity)

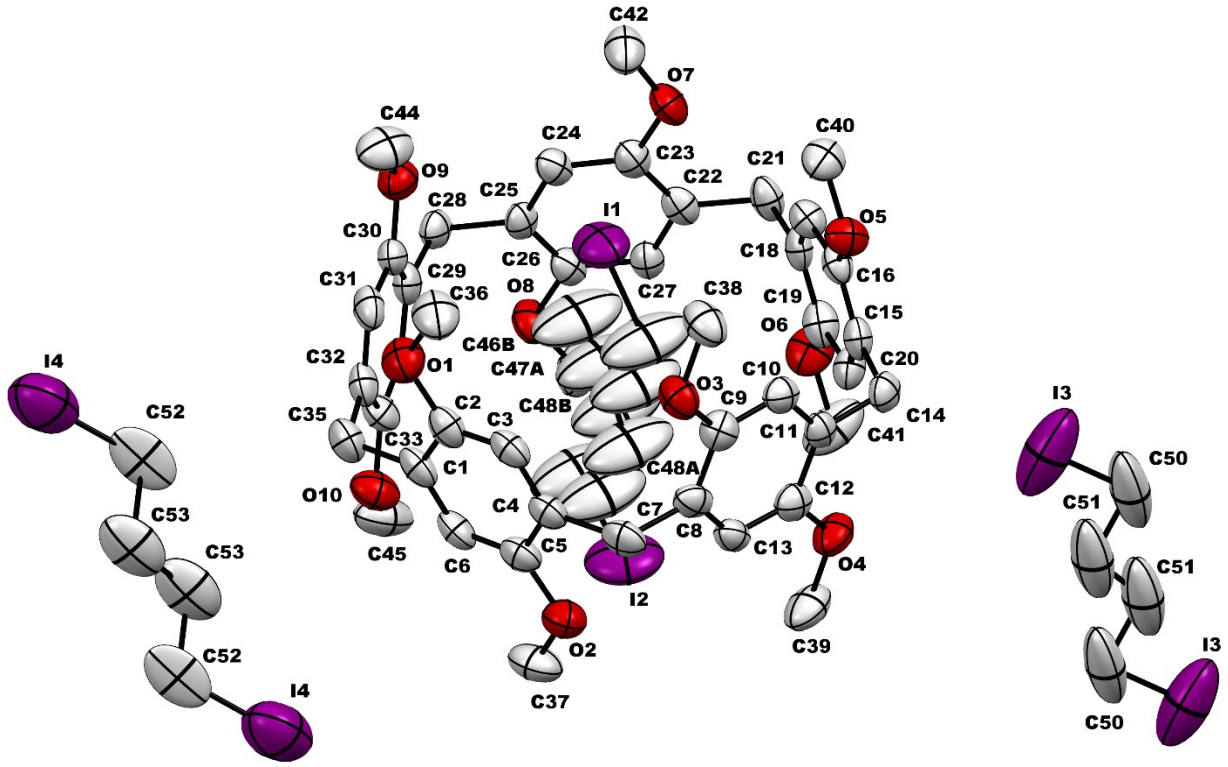

Figure S4. Thermal ellipsoid representation (30% probability) **of** DPM5⊃BuI2 crystal (Hydrogen atoms are hided for clarity).

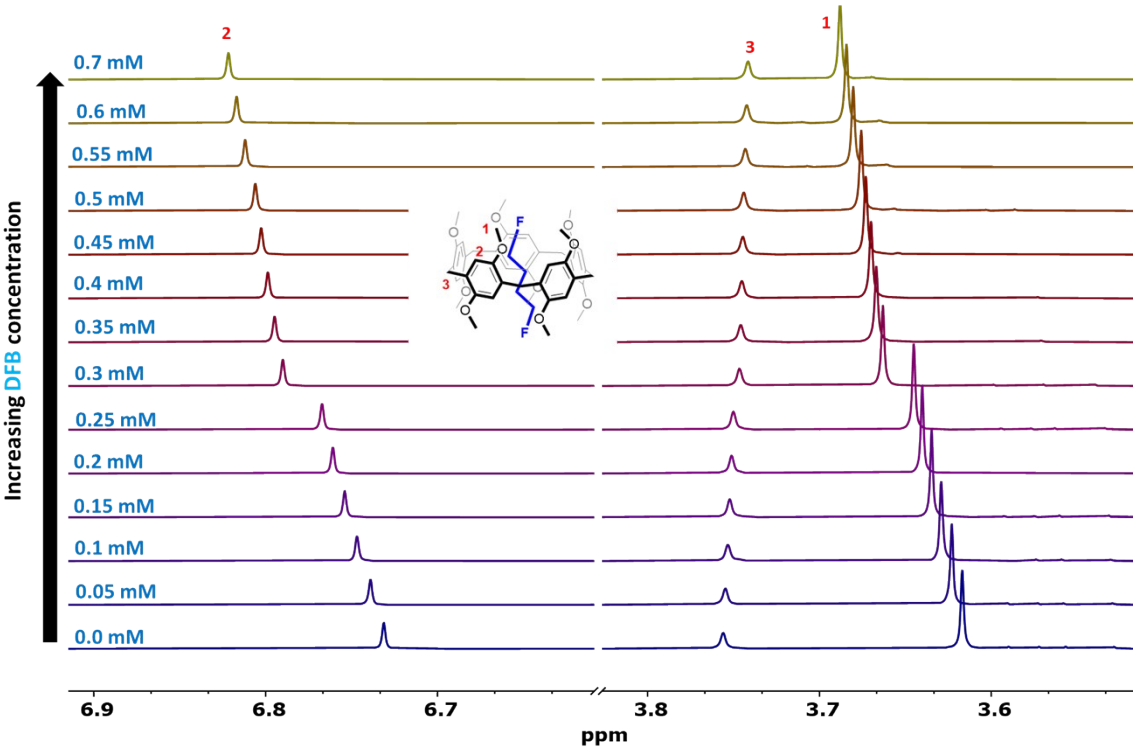

Figure S5. Expanded ^{1}H-NMR (600 MHz, $CDCl_3$, 298 K) spectra of **DMP5** (5 mM) with increasing equimolar quantities (0 →1.4 eq.) of 1,4-difluorobutane (**DFB**).

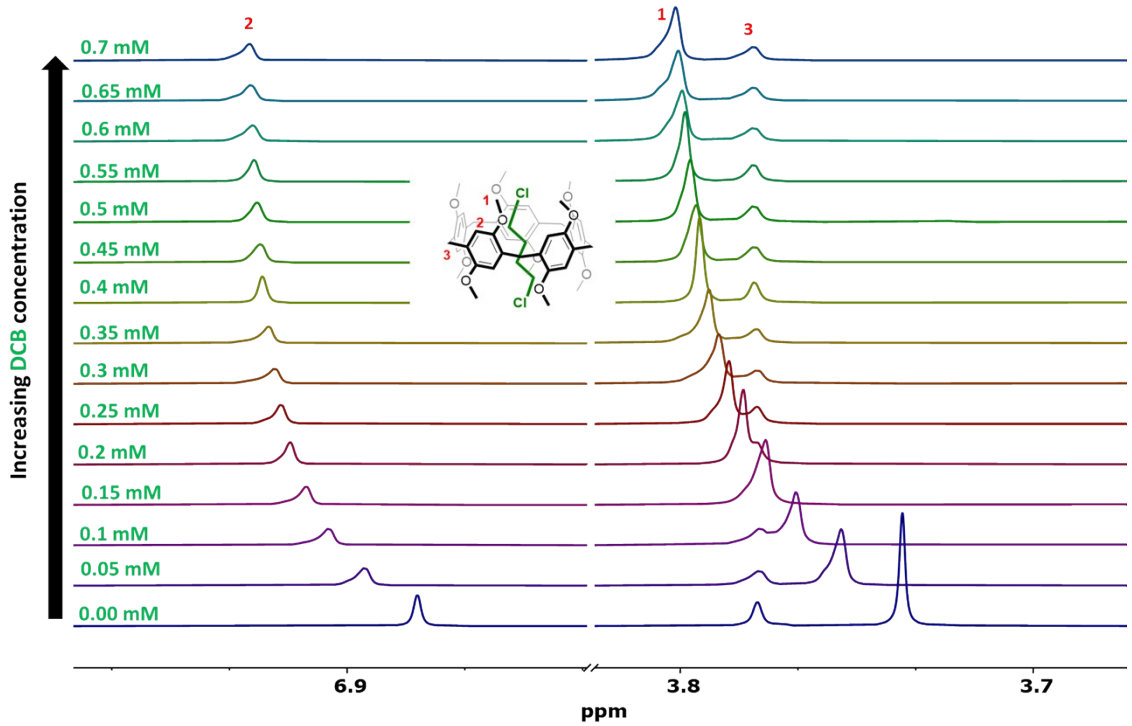

Figure S6. Expanded ^{1}H-NMR (600 MHz, $CDCl_3$, 298 K) spectra of **DMP5** (5 mM) with increasing equimolar quantities (0 →1.4 eq.) of 1,4-dichlorobutane (**DCB**).

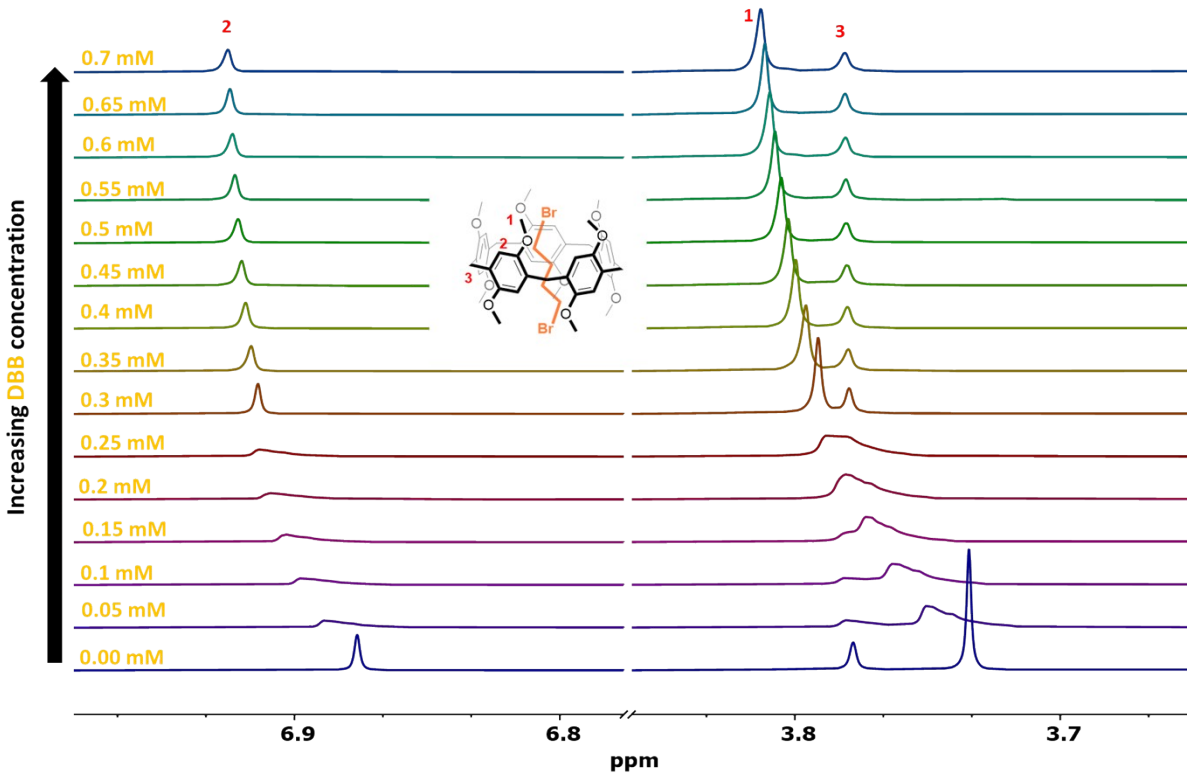

Figure S7. Expanded ^{1}H-NMR (600 MHz, $CDCl_3$, 298 K) spectra of **DMP5** (5 mM) with increasing equimolar quantities (0 →1.4 eq.) of 1,4-dibromobutane (**DBB**).

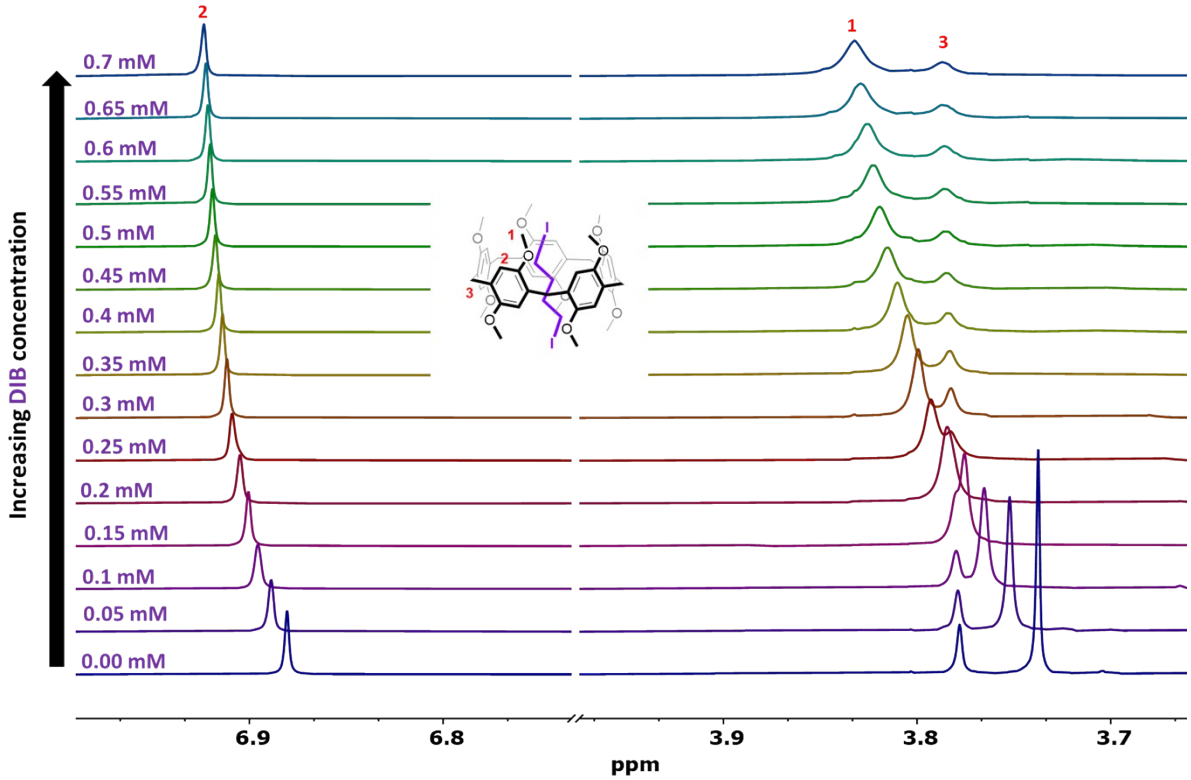

Figure S8. Expanded ^{1}H-NMR (600 MHz, $CDCl_3$, 298 K) spectra of **DMP5** (5 mM) with increasing equimolar quantities (0 →1.4 eq.) of 1,4-diiodobutane (**DIB**).

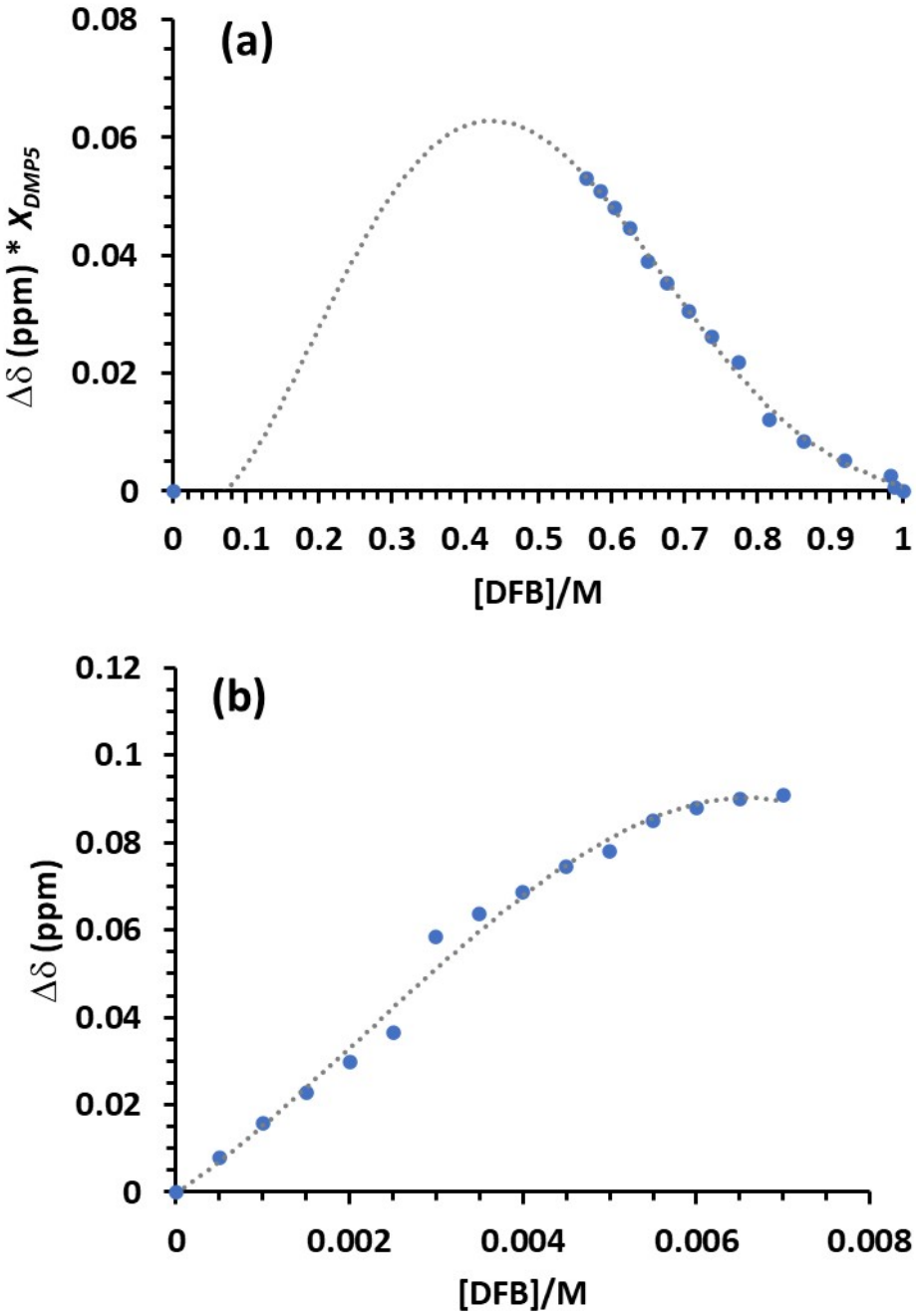

Figure S9. Job's plot for complexation of **DMP5** with 1,4-difluorobutane (**DFB**) guest **(a)**, and plot of chemical shift (δ) changes for the host (**DMP5**) aromatic proton at 6.78 ppm as function of guest (**DFB**) concentration **(b)** determined from ^{1}H-NMR titration $CDCl_3$ at 25 °C.

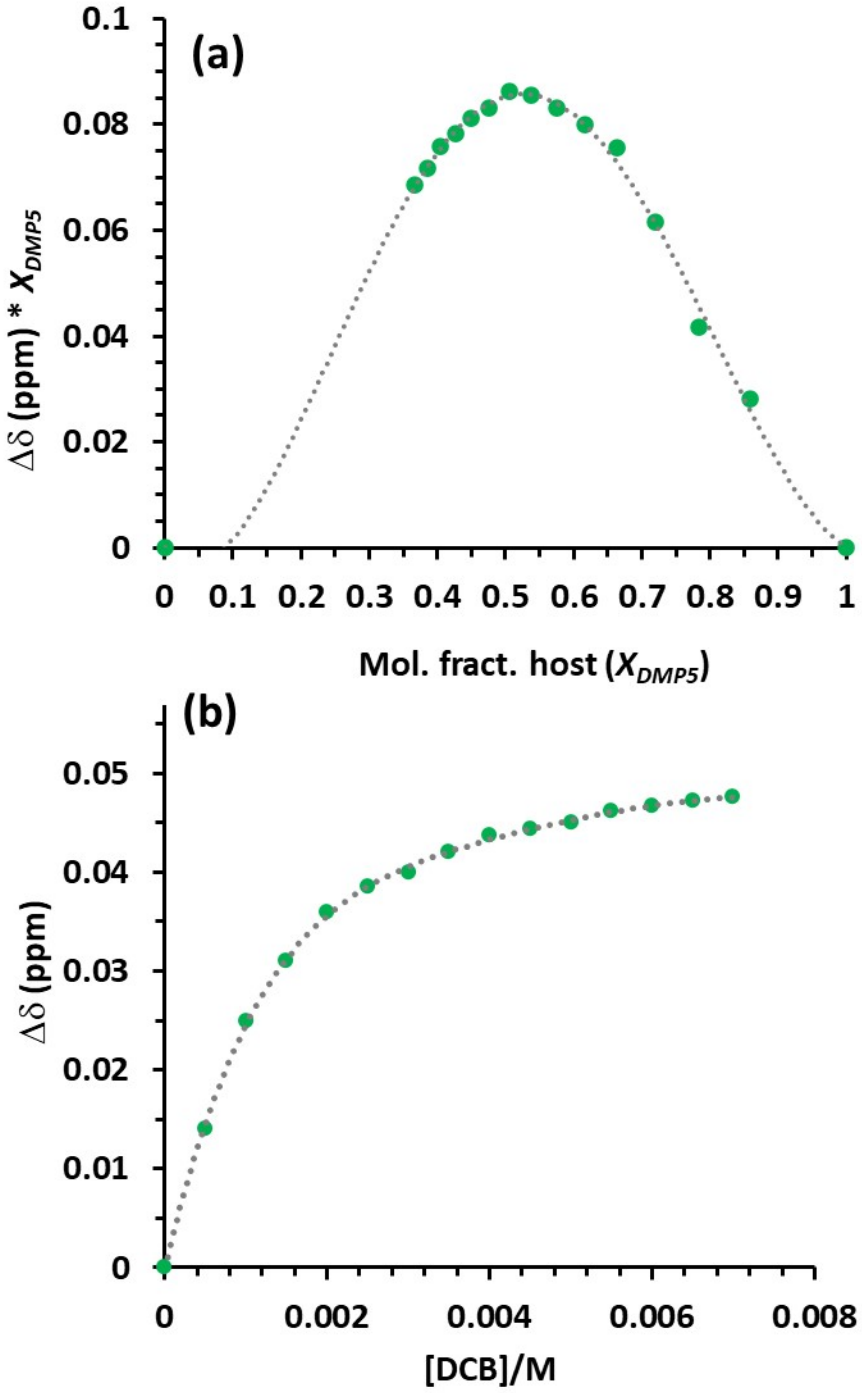

Figure S10. Job's plot for complexation of **DMP5** with 1,4-dichlorobutane (**DCB**) guest **(a)**, and plot of chemical shift (δ) changes for the host (**DMP5**) aromatic proton at 6.78 ppm as function of guest (**DCB**) concentration **(b)** determined from ^{1}H-NMR titration $CDCl_3$ at 25 °C.

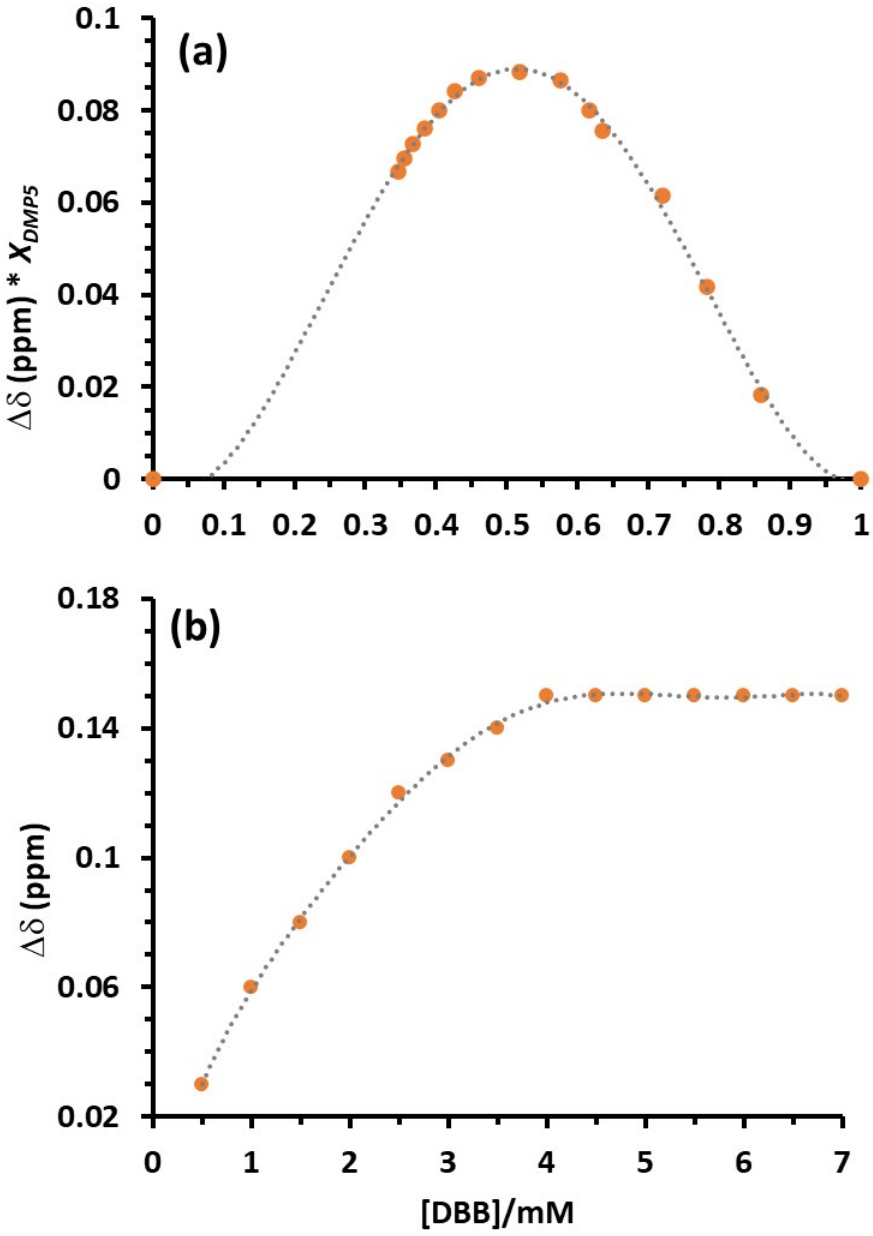

Figure S11. Job's plot for complexation of **DMP5** with 1,4-dibromobutane (**DBB**) guest **(a)**, and plot of chemical shift (δ) changes for the host (**DMP5**) aromatic proton at 6.78 ppm as function of guest (**DBB**) concentration **(b)** determined from ^{1}H-NMR titration $CDCl_3$ at 25 °C.

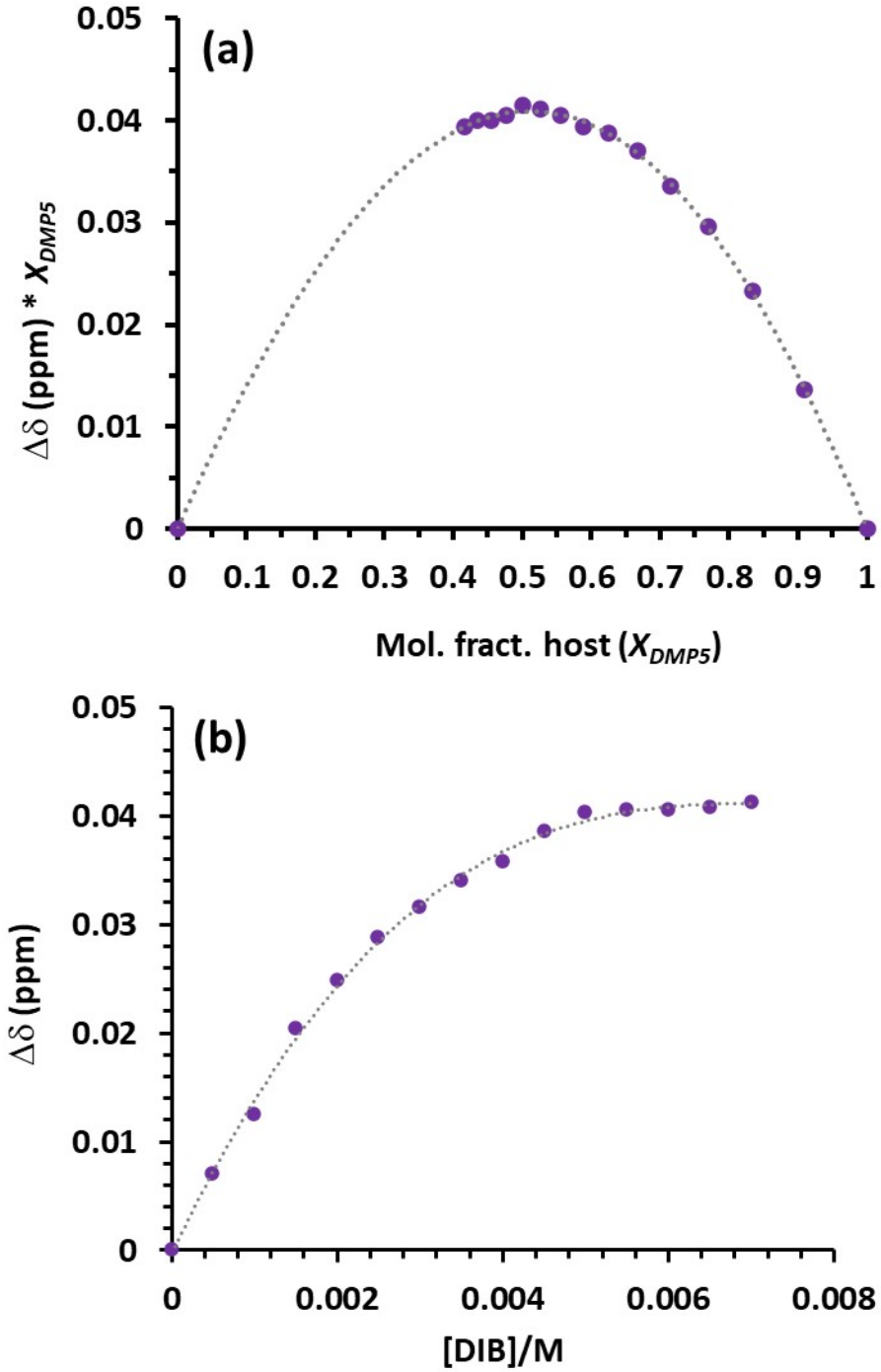

Figure S12. Job's plot for complexation of **DMP5** with 1,4-diodobutane (**DIB**) guest **(a)**, and plot of chemical shift (δ) changes for the host (**DMP5**) aromatic proton at 6.78 ppm as function of guest (**DIB**) concentration **(b)** determined from ^{1}H-NMR titration $CDCl_3$ at 25 °C.

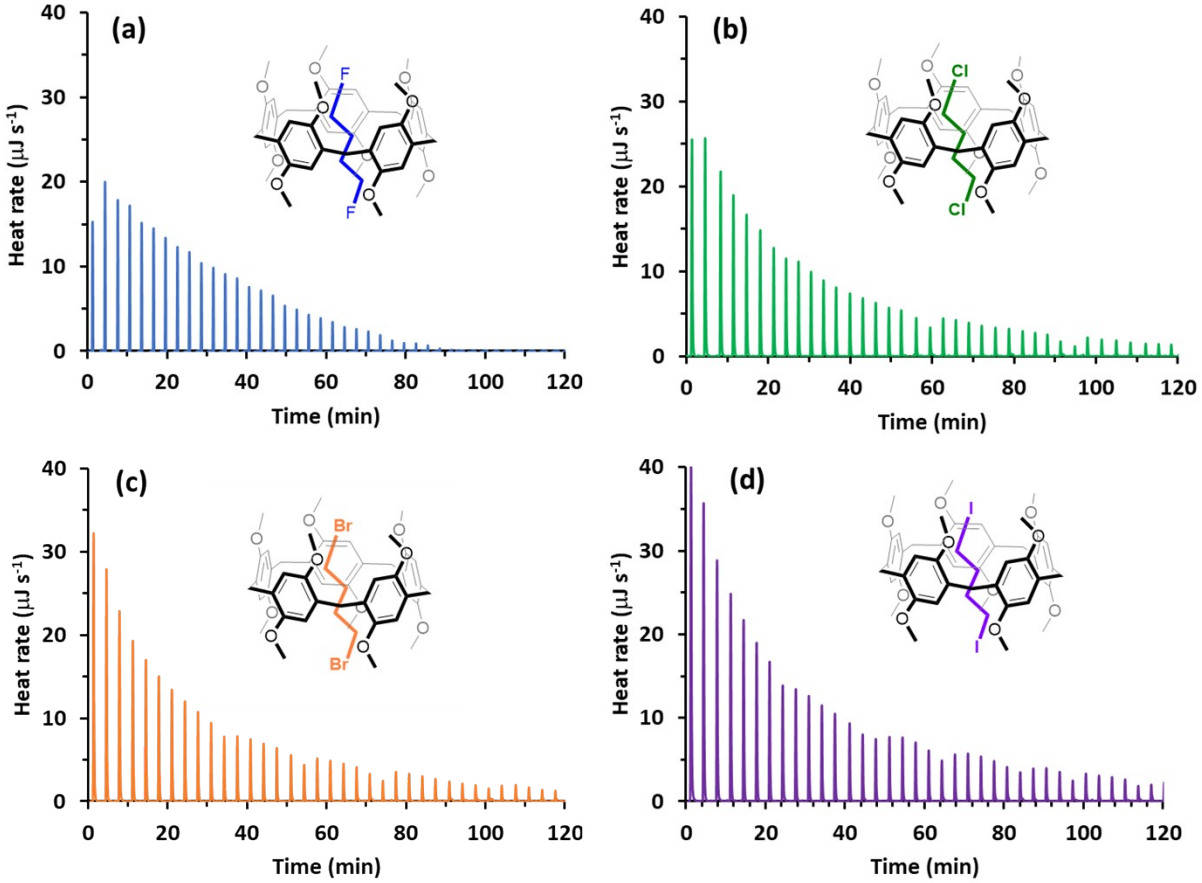

Figure S13. Host-guest complexation ITC experiment raw heats for sequential injections at 25 °C in chloroform for 5 mM **DMP5 host** with 1,4-difluorobutane (**DFB**) (a), 1,4-dichlorobutane (**DCB**) (b), 1,4-dibromobutane (**DBB**) (c), and 1,4-diiodoobutane (**DIB**) (d).

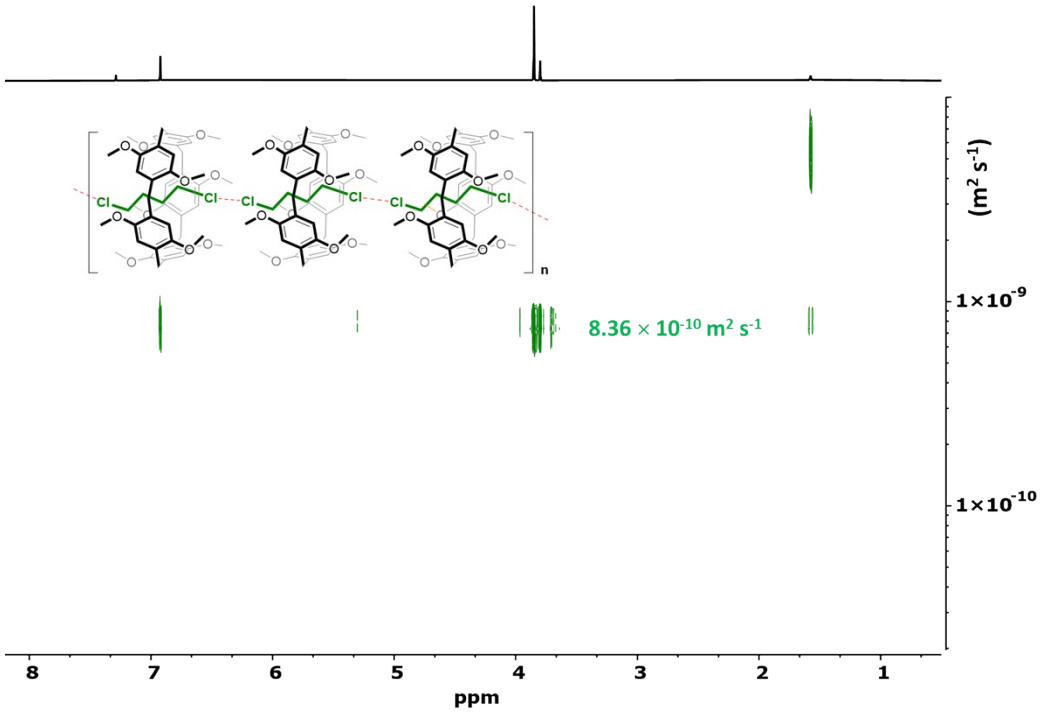

Figure S14. 2D-DOSY spectrum (600 MHz, $CDCl_3$, 298 K) for a 5 mM solution of [**DMP5** ⊃ **DCB**].

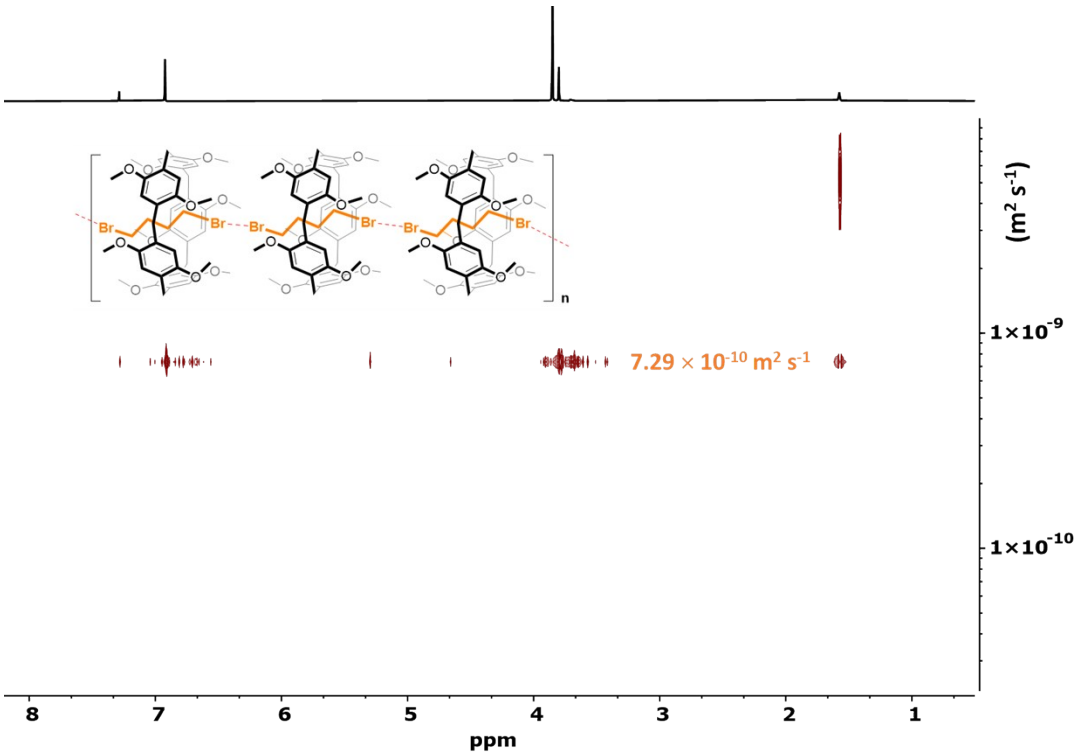

Figure S15. 2D-DOSY spectrum (600 MHz, $CDCl_3$, 298 K) for a 5 mM solution of [**DMP5** ⊃ **DBB**].

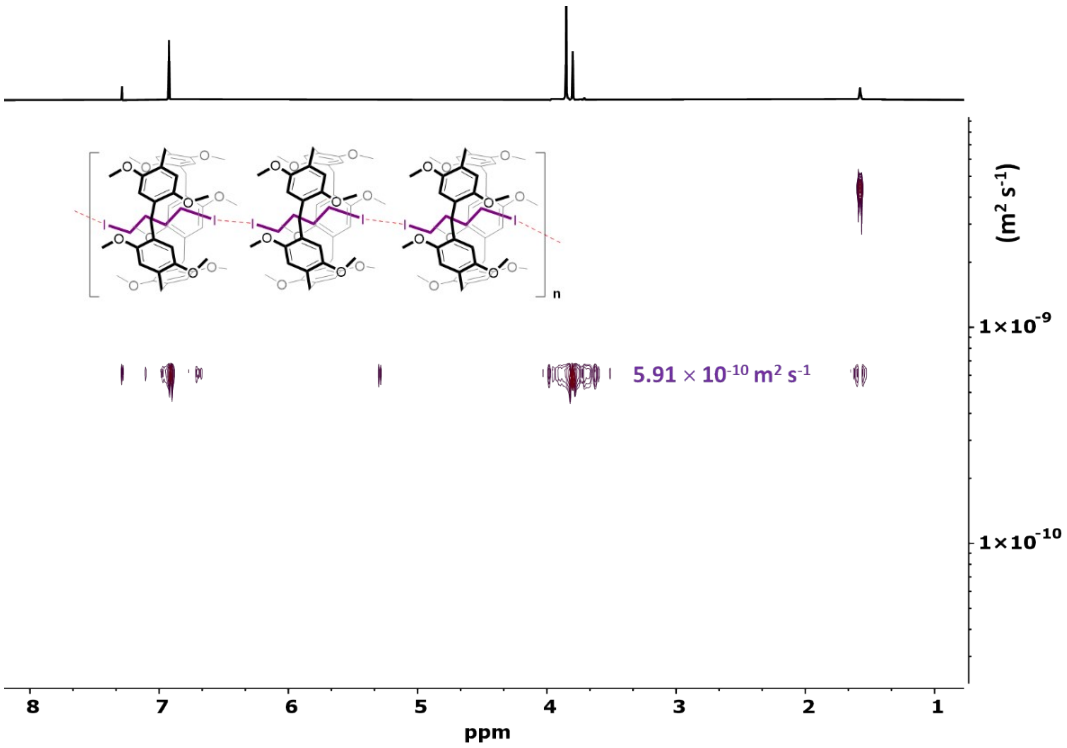

Figure S16. 2D-DOSY spectrum (600 MHz, $CDCl_3$, 298 K) for a 5 mM solution of [**DMP5** ⊃ **DIB**].

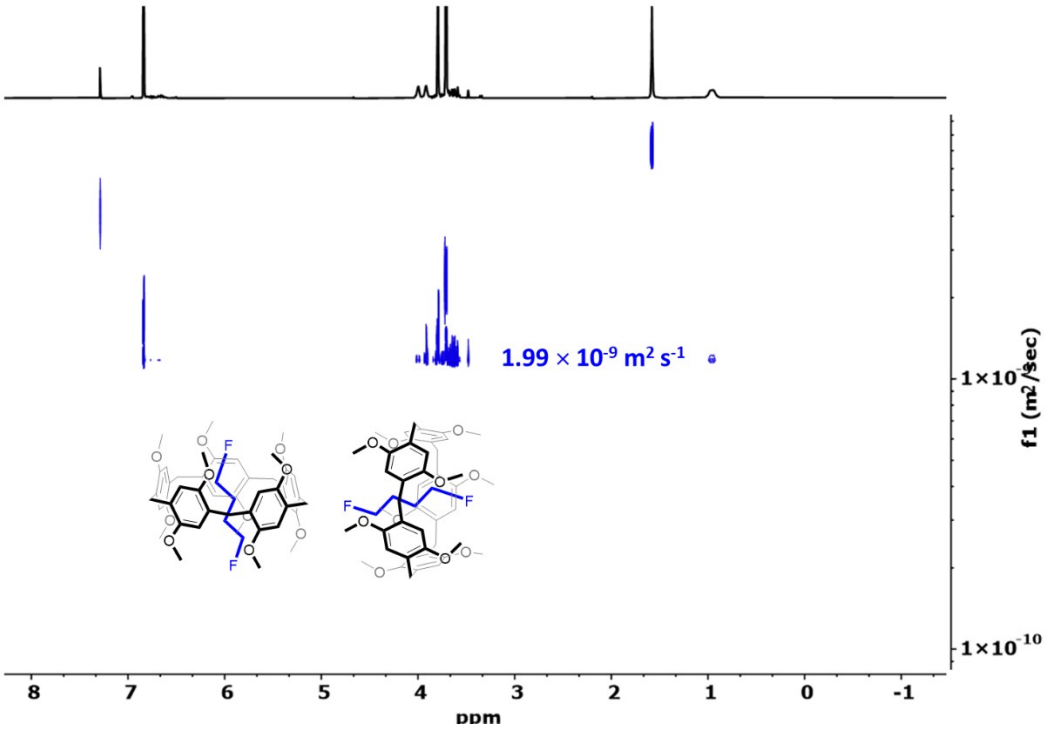

Figure S17. 2D-DOSY spectrum (600 MHz, $CDCl_3$, 298 K) for a 5 mM solution of [**DMP5** ⊃ **DFB**].

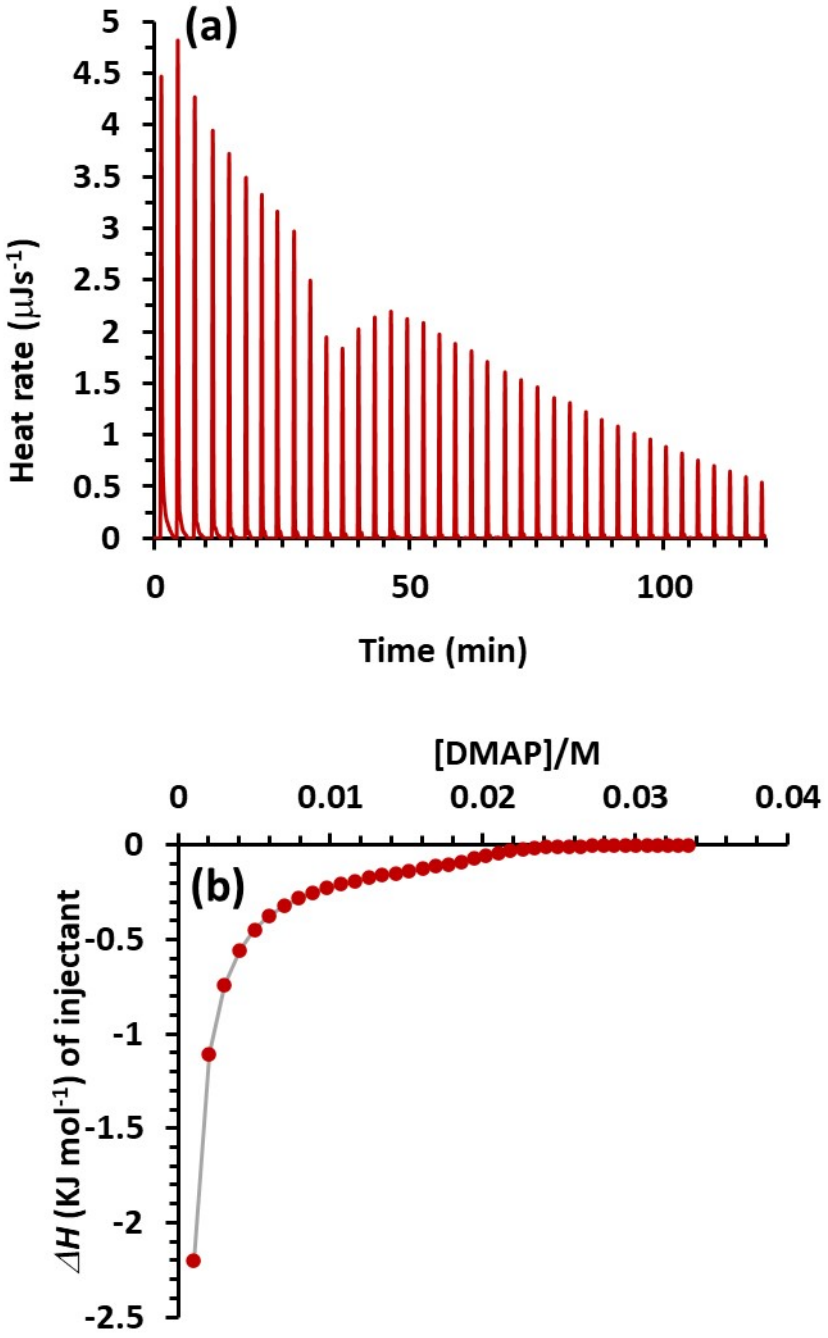

Figure S18. (a) ITC experiment raw heats for sequential injections in chloroform inclusion complex **[DMP5 ⊃ DIB]** with 4-dimethylaminopyrydine (**DMAP**) at 25 °C.(b) Net heat of dissociation of 10 mM solutions of [**DMP5 ⊃ DIB**] promoted by 4-dimethylaminopyrydine (**DMAP**) as a function of concentration (M) after subtracting the heat of dilution.

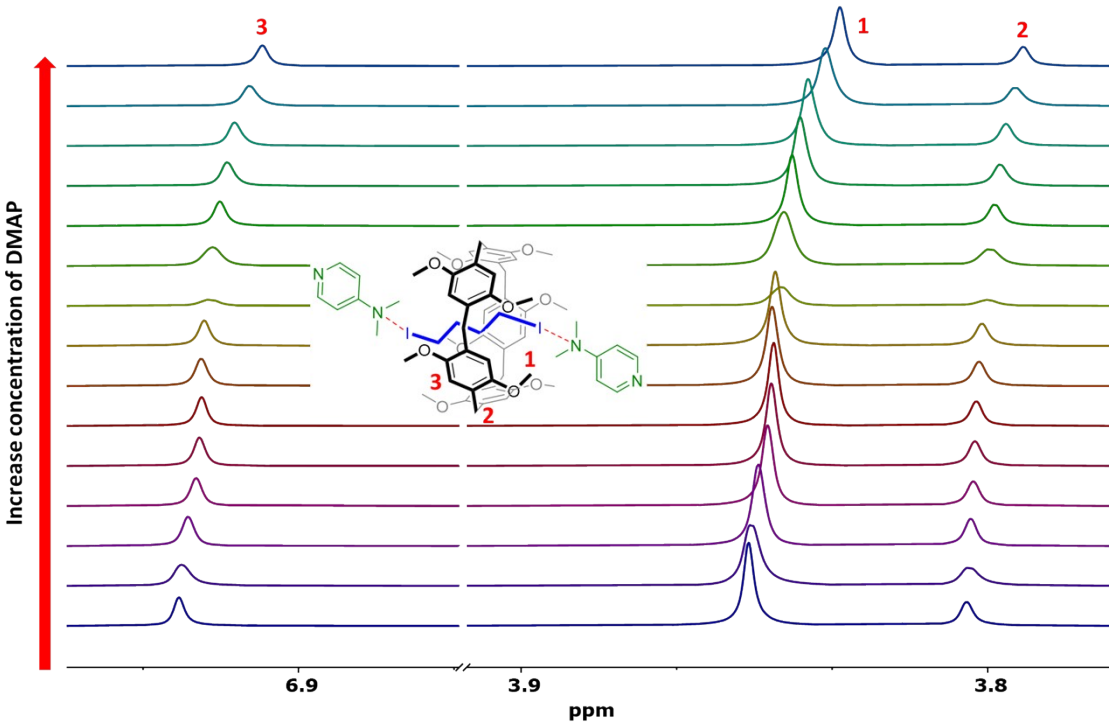

Figure S19. Expanded ^{1}H-NMR (600 MHz, $CDCl_3$, 298 K) spectra of [**DMP5 ⊃ DIB**] (10 mM) with increasing equimolar quantities (0 →10 eq.) of 4-dimethylaminopyrydine (**DMAP**).

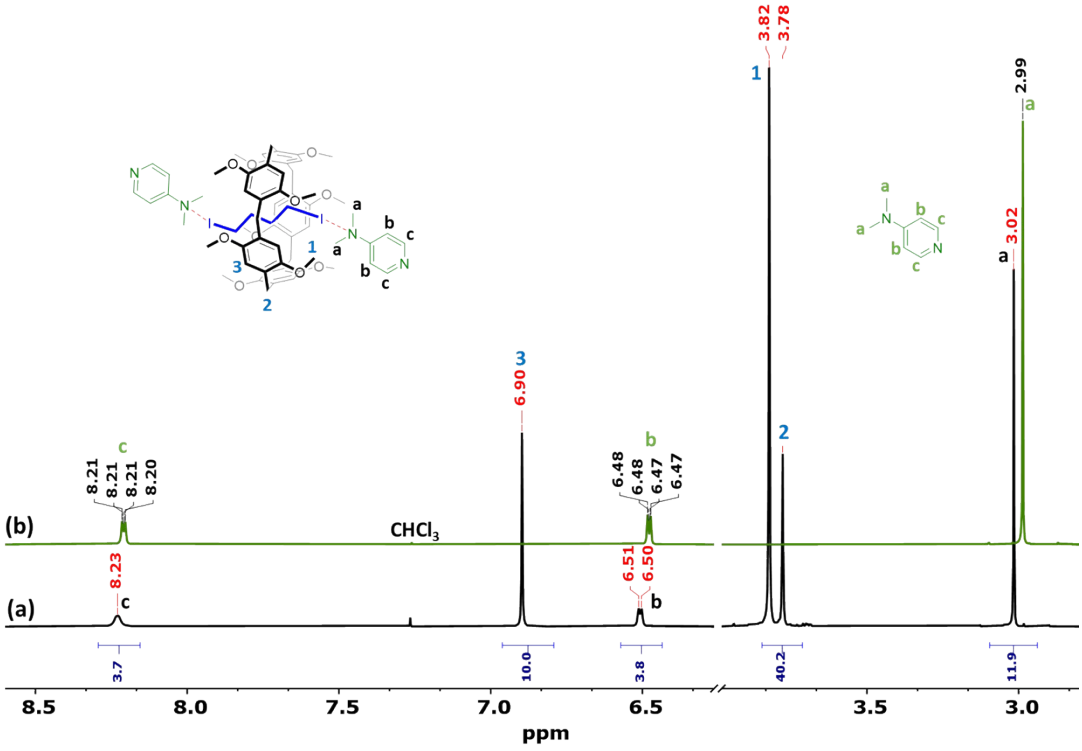

Fig. 20. ^{1}H NMR (600 MHz, chloroform-*d*, 298 K) spectra of [**DMP5 ⊃ DIB**] with 2 equivalents quantity of **DMAP** (a), and **DMAP** alone (b).

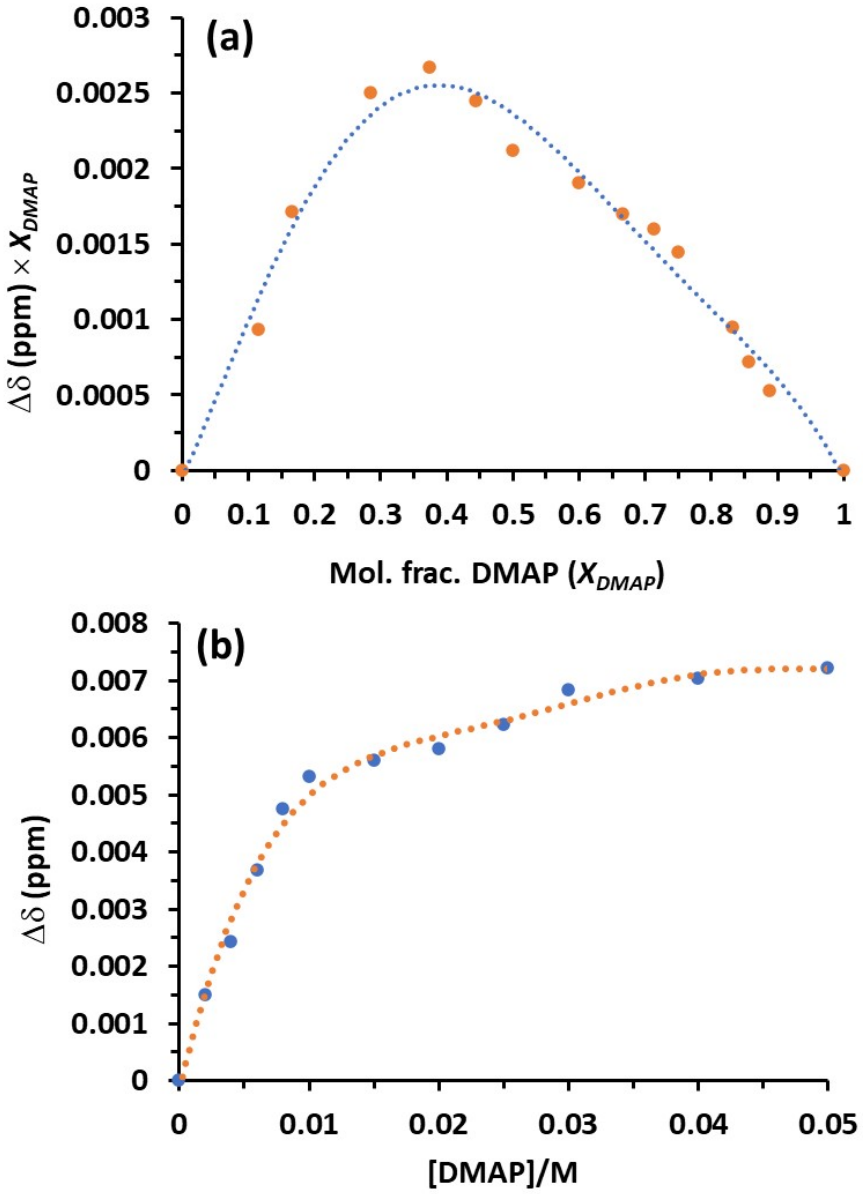

Figure S21. Job's plot for complexation of [**DMP5 ⊃ DIB**] with 4-dimethylaminopyrydine (**DMAP**) **(a)**, and plot of chemical shift (δ) changes for the host [**DMP5 ⊃ DIB**] aromatic proton at 8.15 ppm as function of (**DMAP**) concentration **(b)** determined from ^{1}H-NMR titration $CDCl_3$ at 25 °C.